


## Oscillatory multipulsons: Dissipative soliton trains in bistable reaction-diffusion systems with cross diffusion of attractive-repulsive type

Evgeny P. Zemskov<sup>1,\*</sup>, Mikhail A. Tsyganov<sup>2,†</sup> and Werner Horsthemke<sup>3,‡</sup>

<sup>1</sup>*Federal Research Center for Computer Science and Control, Russian Academy of Sciences, Vavilova 40, 119333 Moscow, Russia*

<sup>2</sup>*Institute of Theoretical and Experimental Biophysics, Russian Academy of Sciences, Institutskaya 3, 142290 Pushchino, Moscow Region, Russia*

<sup>3</sup>*Department of Chemistry, Southern Methodist University, Dallas, Texas 75275-0314, USA*

 (Received 18 December 2019; revised manuscript received 31 January 2020; accepted 24 February 2020; published 12 March 2020)

One-dimensional localized sequences of bound (coupled) traveling pulses, wave trains with a finite number of pulses, are described in a piecewise-linear reaction-diffusion system of the FitzHugh-Nagumo type with linear cross-diffusion terms of opposite signs. The simplest case of two bound pulses, the paired-pulse waves (pulse pairs), is solved analytically. The solutions contain oscillatory tails in the wave profiles so that the pulse pairs consist of a double-peak core and wavy edges. Several pulse pairs with different profile shapes and propagation speeds can appear for the same parameter values of the model when the cross diffusion is dominant. The more general case of many bound pulses, multipulse waves, is studied numerically. It is shown that, dependent on the values of the cross-diffusion coefficients, the multipulse waves upon collision can pass through one another with unchanged size and shape, exhibiting soliton behavior. Moreover, multipulse collisions with the system boundaries can generate a rich variety of wave transformations: the transition from the multipulse waves to pulse-front waves and further to simple fronts or to annihilation as well the transition to solitary pulses or to multipulse waves with lower numbers of pulses. Analytical and numerical results for the pulse pairs agree well with each other.

DOI: [10.1103/PhysRevE.101.032208](https://doi.org/10.1103/PhysRevE.101.032208)

### I. INTRODUCTION

Wave interaction in nonlinear reaction-diffusion systems leads to a rich diversity of pattern formation phenomena with complex behavior and morphology of the emerging structures. Such patterns usually develop in bistable and excitable systems where they result from front and pulse interactions, respectively. The appearance of multiple fronts enables the formation of persistent patterns rather than transient ones [1]. Depending on model parameters, there exists a transition from oscillating (or breathing) patterns to traveling ones [1]. The interaction of a front and a back leads to the formation of various bound structures with a pulse-type shape [1,2]. When the front and the back are following one another, and the back propagates faster than the front, they may form a traveling pulse wave [1]. The interaction of front and back is weak if they are separated by more than a front width [2].

Depending on the type of coupling, oscillations can appear near the front and play the role of inhomogeneities, which stop the propagation of the front giving rise to bound states [2]. The bound state may represent a motionless domain or exhibit a breathing motion or a spatiotemporal pattern resulting from an elasticlike collision of the domain boundaries [3]. The conditions for which the boundaries do not annihilate upon

collision but behave as if they are elastic objects as opposed to the fusion of two pulses and the formation of one wide motionless pulse [4] have been found for front collisions [3] and for pulse collisions [4]. Another particular behavior of pulse interactions upon collision where the solitary pulses pass through one another unchanged was discovered in 1965 and was called soliton interaction [5]. Such solitons appear also in reaction-diffusion equations [6] and in other dissipative systems [7]; they are called dissipative solitons [8,9] or autosolitons [2,10].

In many multicomponent reaction-diffusion systems, a gradient in the concentration of one species induces also a flux of another species so that there exist self-diffusion and cross-diffusion transport processes. The cross-diffusion mechanism can arise from both attractive-attractive and attractive-repulsive interactions. The cross-diffusion terms then have the same or opposite signs, respectively. The case of cross-diffusion terms with opposite signs [11–14] in a two-component system,

$$\frac{\partial u}{\partial t} = f(u, v) + D_1 \frac{\partial^2 u}{\partial x^2} + h_1 \frac{\partial^2 v}{\partial x^2}, \quad (1a)$$

$$\frac{\partial v}{\partial t} = g(u, v) + D_2 \frac{\partial^2 v}{\partial x^2} - h_2 \frac{\partial^2 u}{\partial x^2}, \quad (1b)$$

where  $D_{1,2}$  and  $h_{1,2}$  are the self-diffusion and cross-diffusion coefficients, respectively, and  $f(u, v)$  and  $g(u, v)$  are the kinetic rate terms is equivalent to a nonlinear Schrödinger equation for the complex  $\psi$  function. Such a system is consistent

\*[http://www.researchgate.net/profile/Evgeny\\_Zemskov](http://www.researchgate.net/profile/Evgeny_Zemskov)

†[ttsyganov@iteb.ru](mailto:ttsyganov@iteb.ru)

‡[whorsthe@mail.smu.edu](mailto:whorsthe@mail.smu.edu)

with oscillatory taxis waves and their ability to reflect from each other [11,15]. In an ecological context, the model with cross-diffusion terms with opposite signs describes a pursuit-evasion process in population dynamics with positive taxis of predators up the gradient of prey (pursuit) and negative taxis of prey down the gradient of predators (evasion) [11]. For example, if the nonlinearity of the reaction functions  $f(u, v)$  and  $g(u, v)$  is chosen as in Ref. [11], which corresponds to the Truscott-Brindley model [16], the reaction-diffusion system with cross diffusion describes the population dynamics of phytoplankton ( $u$ ) and zooplankton ( $v$ ).

The magnitude of the cross-diffusion coefficients can be quite large compared to that of the self-diffusion coefficients [17]. It, thus, is reasonable to consider models with strong cross diffusion where the self-diffusion coefficients vanish [18–20] or are small in magnitude. Cross-diffusion-induced spatial, temporal, and spatiotemporal patterns appear in many such systems [21–25]. The basic spatiotemporal patterns, traveling waves caused by cross diffusion [26–29], are the subject of our paper. Pulse waves [20,30] and pulse-front waves [31] in the piecewise-linear FitzHugh-Nagumo (FHN) [32,33] model with linear cross-diffusion terms were investigated previously. The FHN equations, also called the Bonhoeffer–van der Pol [34–36] model, were originally formulated as a simplification of the Hodgkin-Huxley model [37] describing the action potential across a nerve membrane. In this context, the cross-diffusion mechanism reflects the effect of a generic drug on the neuron firing process when the influence of certain drugs or external chemicals alters the normal dynamics of the action potential, so that the spatial propagation of neuron firing is essentially caused by the cross diffusion [28].

The piecewise-linear approximation of the nonlinear kinetic rate terms allows us to perform analytical calculations for the traveling waves. Since the pioneering works by McKean [38] and Rinzel and Keller [39], one usually employs a two-piece approximation for the cubic nonlinearity in the FHN model [40,41], which can be extended to many other nonlinear systems [42–45].

The paper is organized as follows. We describe analytically the paired-pulse waves in Sec. II. In Sec. III, we provide illustrative examples and discuss their profile shapes. In Sec. IV, we show the results of numerical simulations for the propagation behavior of the waves and their interaction with the system boundaries and with each other. We summarize our results in Sec. V.

## II. MODEL AND SOLUTIONS

The FHN model is a system of two reaction-diffusion equations where the variable  $u = u(x, t)$  represents the “activator” or potential variable, and the variable  $v = v(x, t)$  represents the “inhibitor” or recovery variable. The FHN model with linear cross-diffusion terms, reflecting attractive-repulsive interactions, is described by equations [15,18,46],

$$\frac{\partial u}{\partial t} = u(1-u)(u-a) - v + D_1 \frac{\partial^2 u}{\partial x^2} + h_1 \frac{\partial^2 v}{\partial x^2}, \quad (2a)$$

$$\frac{\partial v}{\partial t} = \varepsilon(u-v) + D_2 \frac{\partial^2 v}{\partial x^2} - h_2 \frac{\partial^2 u}{\partial x^2}, \quad (2b)$$

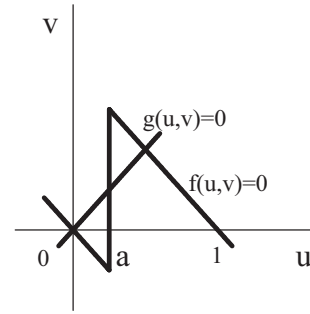


FIG. 1. The nullclines  $f(u, v) = -u - v + H(u - a) = 0$  and  $g(u, v) = u - v = 0$ .

where the parameters  $a$  and  $\varepsilon$  are the excitation threshold and the ratio of timescales, respectively. We consider here the piecewise-linear approximation [18,39],

$$\frac{\partial u}{\partial t} = -u - v + H(u - a) + D_1 \frac{\partial^2 u}{\partial x^2} + h_1 \frac{\partial^2 v}{\partial x^2}, \quad (3a)$$

$$\frac{\partial v}{\partial t} = \varepsilon(u - v) + D_2 \frac{\partial^2 v}{\partial x^2} - h_2 \frac{\partial^2 u}{\partial x^2}, \quad (3b)$$

with the Heaviside step function  $H(u - a)$ . The excitation threshold must be  $0 < a < 1/2$  for the system to be bistable. The nullclines  $f(u, v) = -u - v + H(u - a) = 0$  and  $g(u, v) = u - v = 0$  for the bistable regime are shown in Fig. 1.

We look for a specific type of solutions, namely, traveling waves  $u = u(\xi)$  and  $v = v(\xi)$ , where  $\xi = x - ct$  is the traveling frame coordinate and  $c$  is the wave speed. Such solutions represent waves that propagate in space with constant speed and without changing shape. The traveling wave solutions satisfy the ordinary differential equations,

$$D \frac{d^2 u}{d\xi^2} + h \frac{d^2 v}{d\xi^2} + c \frac{du}{d\xi} - u - v + H(u - a) = 0, \quad (4a)$$

$$D \frac{d^2 v}{d\xi^2} - h \frac{d^2 u}{d\xi^2} + c \frac{dv}{d\xi} + u - v = 0. \quad (4b)$$

To solve the model analytically, we consider the cases of  $D_1 = D_2 \equiv D$ ,  $h_1 = h_2 \equiv h$ , and  $\varepsilon = 1$ . The mathematical details of the general solutions for traveling waves can be found in Ref. [47].

Here, we focus on the traveling pulse waves. The pulses are homoclinic solutions whose trajectory on the  $(u, v)$ -phase plane starts at a fixed point or steady state as  $\xi \rightarrow -\infty$  and approaches the same fixed point as  $\xi \rightarrow +\infty$ . The well-known standard pulse solutions in the piecewise linear reaction-diffusion model consist of three parts or tails that correspond to the peak and the growing and decaying edges. In this paper, we extend these simple pulses to similar homoclinic solutions that consist of five parts,  $u_{1,\dots,5}$  and  $v_{1,\dots,5}$ . The edge pieces of these waves,  $u_1, v_1$  and  $u_5, v_5$ , repeat the behavior of the edges of simple pulses, whereas the middle pieces  $u_{2-4}$  and  $v_{2-4}$  form two-peak patterns. This two-peak pattern represents a bound pulse pair, and we will call such waves paired-pulse waves or just pulse pairs. The spatiotemporal pattern illustrating the propagation of the pulse pair for the activator variable  $u(x, t)$  is shown in Fig. 2.

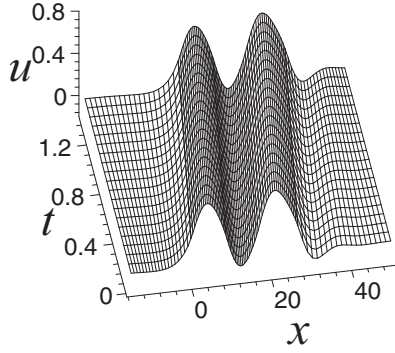


FIG. 2. Space-time plot showing the evolution of the paired-pulse wave for the activator variable  $u(x, t)$ .

The boundary conditions for the pulses are as follows,  $u_1, v_1(\xi \rightarrow -\infty) = u_5, v_5(\xi \rightarrow +\infty) = 0$  so that the solutions read

$$u_1(\xi) = e^{k_+\xi} [A_{11} \cos(l_-\xi) + A_{13} \sin(l_-\xi)], \quad (5a)$$

$$u_2(\xi) = e^{k_+\xi} [A_{21} \cos(l_-\xi) + A_{23} \sin(l_-\xi)] + e^{k_-\xi} [A_{22} \cos(l_+\xi) + A_{24} \sin(l_+\xi)] + 1/2, \quad (5b)$$

$$u_3(\xi) = e^{k_+\xi} [A_{31} \cos(l_-\xi) + A_{33} \sin(l_-\xi)] + e^{k_-\xi} [A_{32} \cos(l_+\xi) + A_{34} \sin(l_+\xi)], \quad (5c)$$

$$u_4(\xi) = e^{k_+\xi} [A_{41} \cos(l_-\xi) + A_{43} \sin(l_-\xi)] + e^{k_-\xi} [A_{42} \cos(l_+\xi) + A_{44} \sin(l_+\xi)] + 1/2, \quad (5d)$$

$$u_5(\xi) = e^{k_-\xi} [A_{52} \cos(l_+\xi) + A_{54} \sin(l_+\xi)] \quad (5e)$$

for the activator variable, and

$$v_1(\xi) = e^{k_+\xi} [B_{11} \cos(l_-\xi) + B_{13} \sin(l_-\xi)], \quad (6a)$$

$$v_2(\xi) = e^{k_+\xi} [B_{21} \cos(l_-\xi) + B_{23} \sin(l_-\xi)] + e^{k_-\xi} [B_{22} \cos(l_+\xi) + B_{24} \sin(l_+\xi)] + 1/2, \quad (6b)$$

$$v_3(\xi) = e^{k_+\xi} [B_{31} \cos(l_-\xi) + B_{33} \sin(l_-\xi)] + e^{k_-\xi} [B_{32} \cos(l_+\xi) + B_{34} \sin(l_+\xi)], \quad (6c)$$

$$v_4(\xi) = e^{k_+\xi} [B_{41} \cos(l_-\xi) + B_{43} \sin(l_-\xi)] + e^{k_-\xi} [B_{42} \cos(l_+\xi) + B_{44} \sin(l_+\xi)] + 1/2, \quad (6d)$$

$$v_5(\xi) = e^{k_-\xi} [B_{52} \cos(l_+\xi) + B_{54} \sin(l_+\xi)] \quad (6e)$$

for the inhibitor variable. The solution parameters are the same as in Ref. [47]:  $k_{\pm} = \pm y - p$  and  $l_{\pm} = z \pm q$ , where

$$p = \frac{cD}{2(D^2 + h^2)}, \quad q = \frac{ch}{2(D^2 + h^2)}, \quad (7a)$$

$$b = p^2 - q^2 + \frac{p+q}{c/2}, \quad d = 2pq - \frac{p-q}{c/2}, \quad (7b)$$

$$y = \sqrt{(\sqrt{b^2 + d^2} + b)/2}, \quad z = \sqrt{(\sqrt{b^2 + d^2} - b)/2}, \quad (7c)$$

and the integration constants  $B$  are expressed as

$$B_{1,3} = -\frac{(\alpha_1\gamma_1 + \beta_1\delta_1)A_{1,3} \mp (\alpha_1\delta_1 - \beta_1\gamma_1)A_{3,1}}{\gamma_1^2 + \delta_1^2}, \quad (8a)$$

$$B_{2,4} = -\frac{(\alpha_2\gamma_2 + \beta_2\delta_2)A_{2,4} \mp (\alpha_2\delta_2 - \beta_2\gamma_2)A_{4,2}}{\gamma_2^2 + \delta_2^2}, \quad (8b)$$

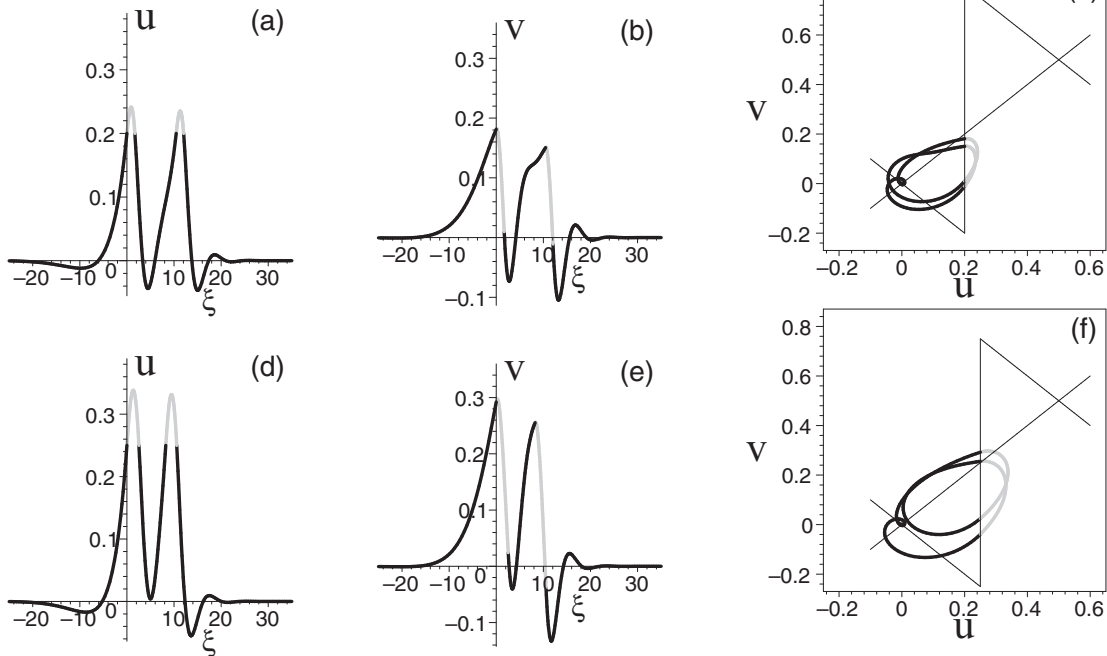


FIG. 3. (a) and (d) Paired-pulse waves for the activator  $u(\xi)$ , (b) and (e) for the inhibitor  $v(\xi)$ , and (c) and (f) on the  $(u, v)$ -phase plane (bold lines) for the model with both self-diffusion and cross-diffusion terms ( $D = 1$ ,  $h = 5$ ): (a)–(c)  $a = 0.2$ ,  $c \approx 5.269$  and (d)–(f)  $a = 0.25$ ,  $c \approx 4.919$ . The parts  $u_2, u_4$  and  $v_2, v_4$  of the waves are shown in gray. The nullclines  $f(u, v) = 0$  and  $g(u, v) = 0$  are shown as thin lines in panels (c) and (f).

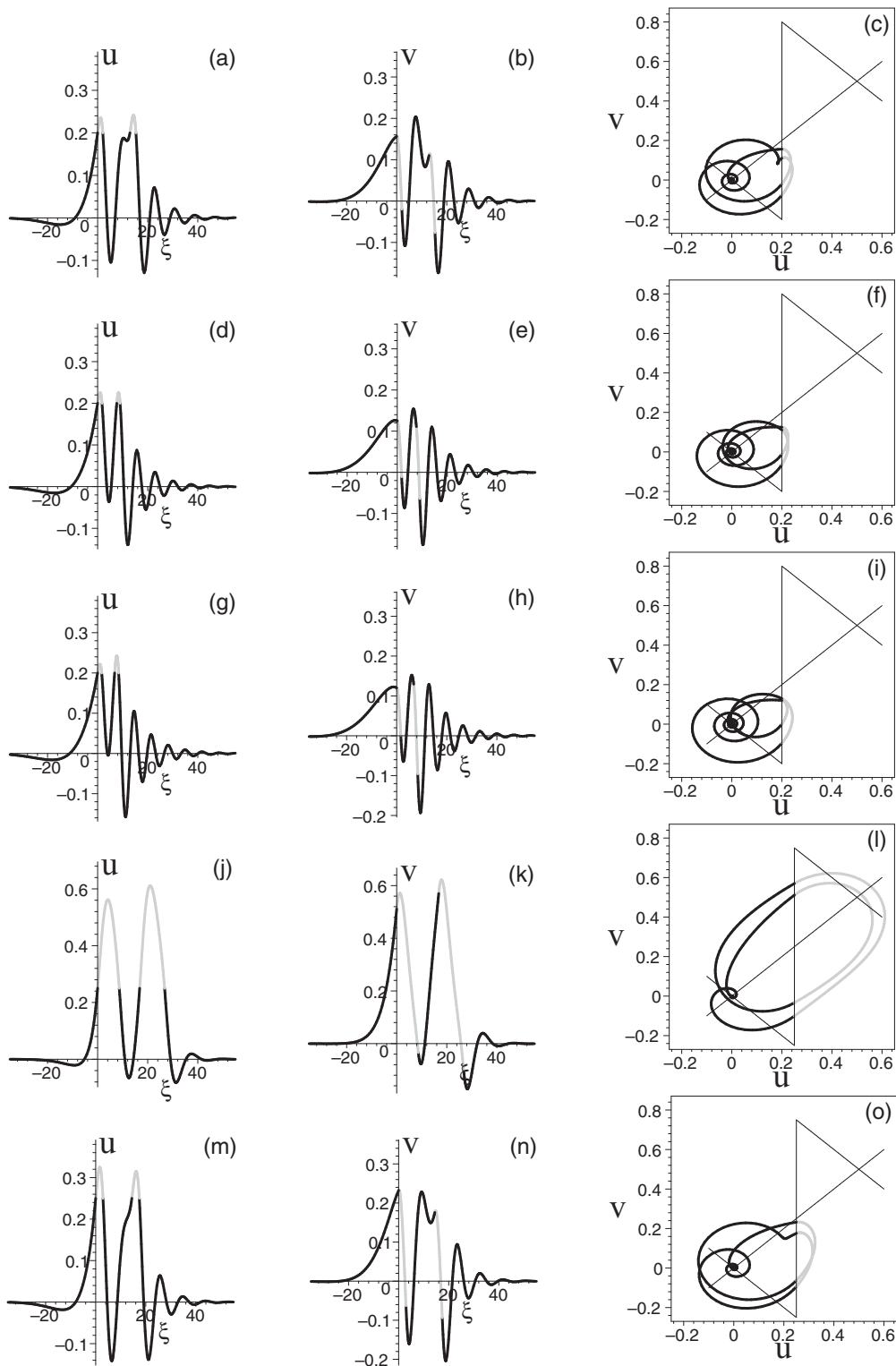


FIG. 4. (a), (d), (g), (j), and (m) Paired-pulse waves for the activator  $u(\xi)$ , (b), (e), (h), (k), and (n) for the inhibitor  $v(\xi)$ , and (c), (f), (i), (l), and (o) on the  $(u, v)$ -phase plane (bold lines) for the model with pure cross-diffusion terms  $D = 0$ ,  $h = 10$ . Panels (a)–(i) correspond to the small threshold  $a = 0.2$ : (a)–(c) the slow wave  $c \approx 8.802$ , (d)–(f) the intermediate wave  $c \approx 9.666$ , and (g)–(i) the fast wave  $c \approx 10.195$ . Panels (j)–(o) correspond to the large threshold  $a = 0.25$ : (j)–(l) the slow wave  $c \approx 5.936$ , and (m)–(o) the fast wave  $c \approx 7.932$ . The parts  $u_2, u_4$  and  $v_2, v_4$  of the waves are shown in gray. The nullclines  $f(u, v) = 0$  and  $g(u, v) = 0$  are shown as thin lines in panels (c), (f), (i), (l), and (o).

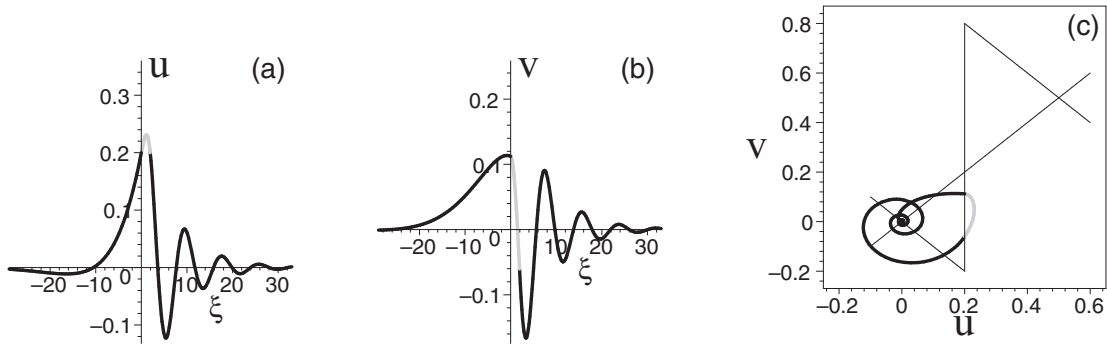


FIG. 5. An example of the solitary pulses: (a) for the activator  $u(\xi)$ , (b) for the inhibitor  $v(\xi)$ , and (c) on the  $(u, v)$ -phase plane (bold lines) for the model with pure cross-diffusion terms  $D = 0$ ,  $h = 10$  for  $a = 0.2$ . The wave speed is  $c \approx 8.723$ . The parts  $u_2$  and  $v_2$  of the waves are shown in gray. The nullclines  $f(u, v) = 0$  and  $g(u, v) = 0$  are shown as thin lines in panels (c).

with

$$\alpha_1 = D(k_+^2 - l_-^2) + ck_+ - 1, \quad \beta_1 = l_-(2Dk_+ + c), \quad (9a)$$

$$\gamma_1 = h(k_+^2 - l_-^2) - 1, \quad \delta_1 = 2hk_+l_-, \quad (9b)$$

$$\alpha_2 = D(k_-^2 - l_+^2) + ck_- - 1, \quad \beta_2 = l_+(2Dk_- + c), \quad (9c)$$

$$\gamma_2 = h(k_-^2 - l_+^2) - 1, \quad \delta_2 = 2hk_-l_+. \quad (9d)$$

The five parts of the pulse profile, (5) and (6), are fitted together using the matching conditions for the pieces  $u_n(\xi)$ ,  $v_n(\xi)$ ,  $n = 1, \dots, 5$ , and their derivatives  $du_n(\xi)/d\xi$ ,  $dv_n(\xi)/d\xi$  at the four matching points. In total, there are 20 equations for 20 unknown constants (16 integration constants  $A$ , three matching point coordinates and the pulse speed  $c$ ), which allows us to determine the pulse speed

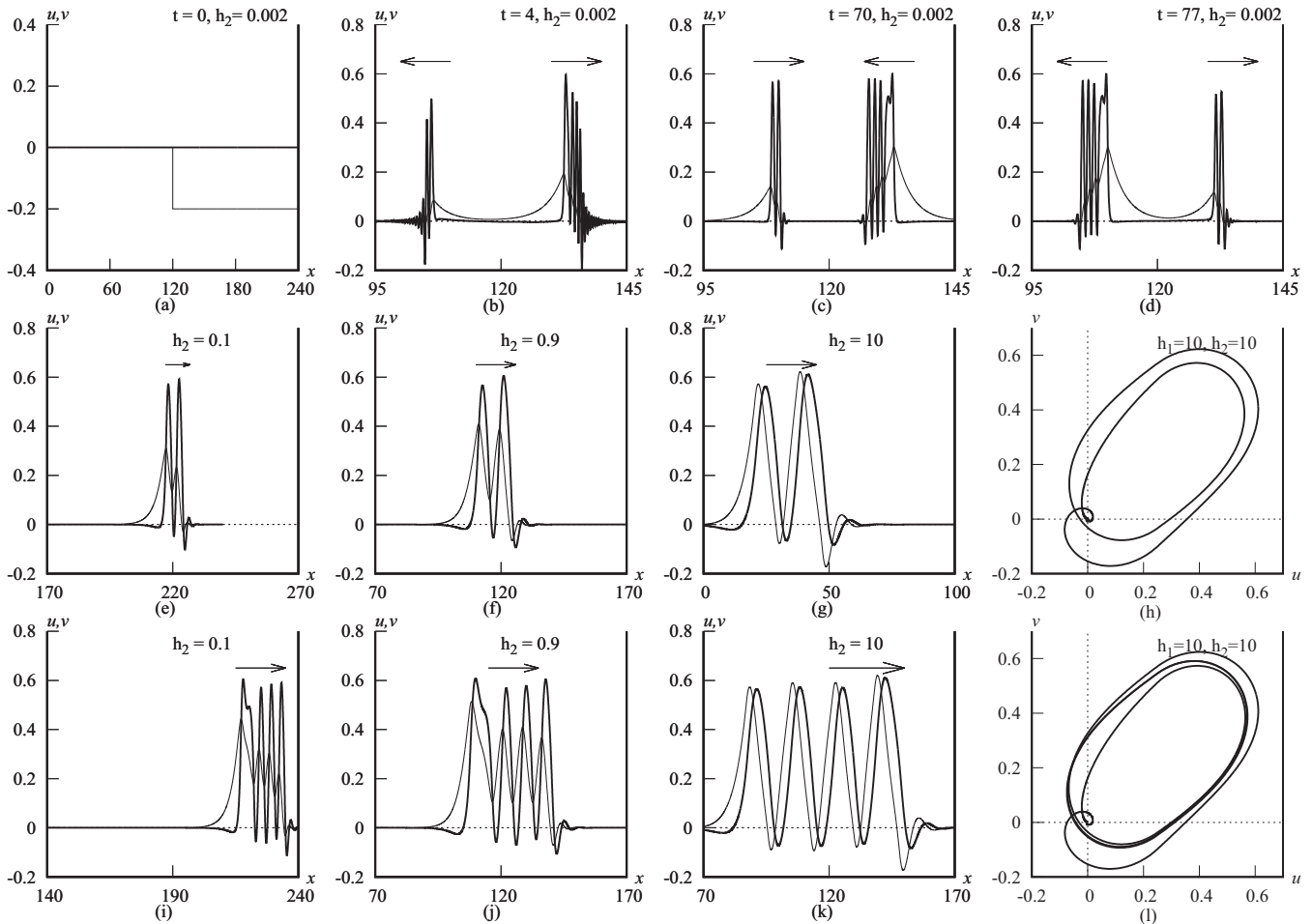


FIG. 6. Numerical simulations. Multipulse waves with two and four peaks for different values of  $h_2$ . The activator  $u(x, t)$  and the inhibitor  $v(x, t)$  are shown in black and gray, respectively. The values of the model parameters are fixed at  $a = 0.25$ ,  $\varepsilon = 1$ ,  $D_1 = D_2 = 0$ , and  $h_1 = 10$ . The size of the medium and the initial constant are chosen as  $L = 240$  and  $v_0 = -0.2$ , respectively. Different panels display different segments of the  $x$  axis to zero on the multipulse waves.

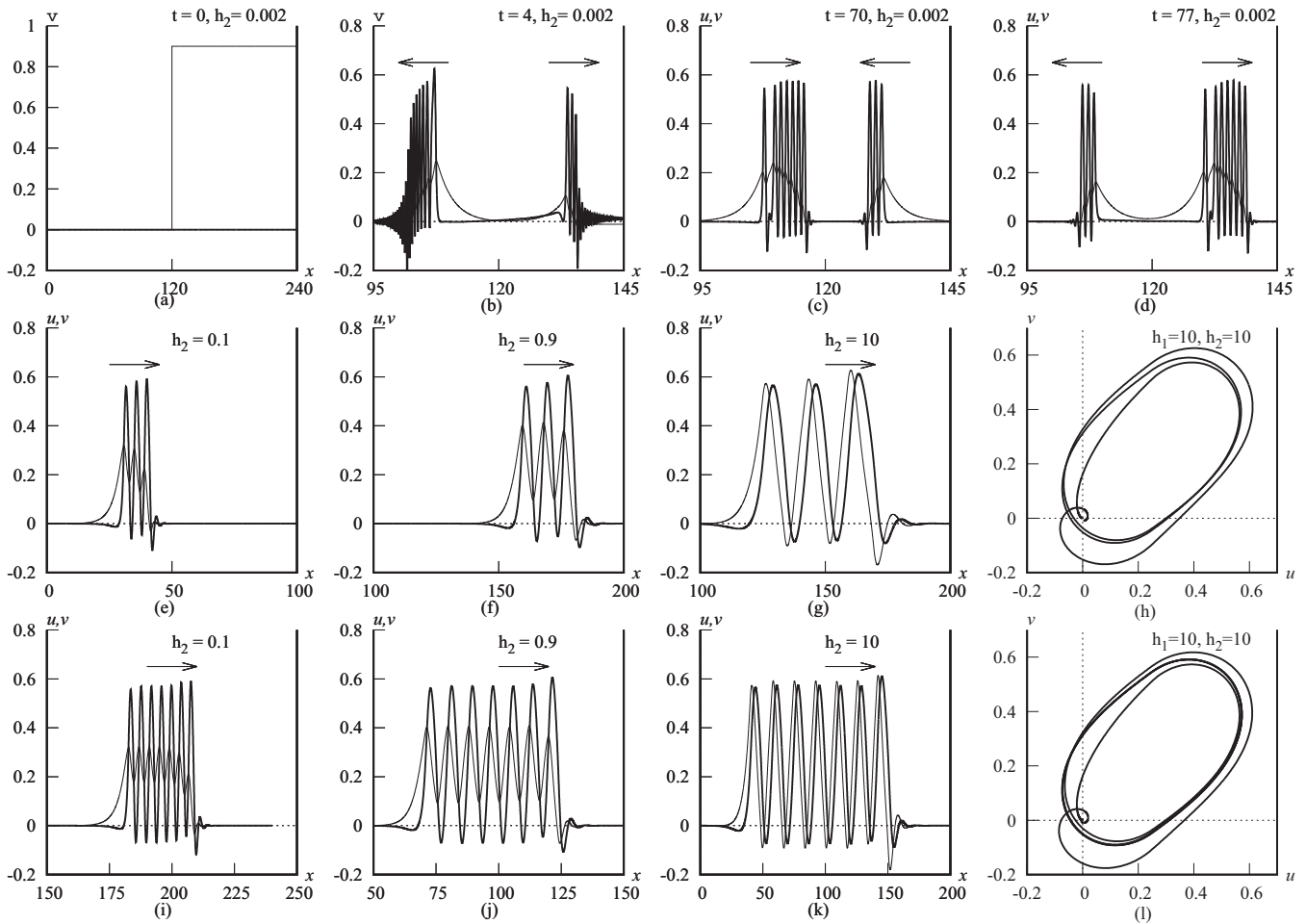


FIG. 7. Numerical simulations. Multipulse waves with three and seven peaks for different values of  $h_2$ . The activator  $u(x, t)$  and the inhibitor  $v(x, t)$  are shown in black and gray, respectively. The values of the model parameters are fixed at  $a = 0.25$ ,  $\varepsilon = 1$ ,  $D_1 = D_2 = 0$ , and  $h_1 = 10$ . The size of the medium and the initial constant are chosen as  $L = 240$  and  $v_0 = 0.9$ , respectively. Different panels display different segments of the  $x$  axis to zero on the multipulse waves.

and the matching points uniquely. The first matching point is chosen to be zero due to the translational invariance of the equations [47].

### III. PAIRED-PULSE WAVES

The results of the analytical calculations for the traveling paired-pulse waves, traveling pulse pairs, are shown graphically in Fig. 3 for the model (4) with both self-diffusion and cross-diffusion terms and in Fig. 4 for the pure cross-diffusion model where the self-diffusion terms vanish. In the first case, the wave profiles display pronounced two pulse peaks. The oscillatory character of the solutions (5) and (6) manifests itself only in the small tails (the oscillations attenuate rapidly) on the leading edges, which are located on the right side of the waves before the peaks. The bound pulse pair, which forms a big double loop on the  $(u, v)$ -phase plane [Figs. 3(c) and 3(f)], consists essentially of the strongly pronounced pulse peaks. In the second case, the pure cross-diffusion model, we observe a so-called *multiwave regime* of propagation for the paired-pulse waves, namely, the simultaneous coexistence of several waves with different profile shapes and propagation speeds for the same values of the model parameters. There exist three

waves with their own profiles and speed values, the slow, intermediate, and fast waves for  $a = 0.2$ , and two waves, the slow and fast waves for  $a = 0.25$  (Fig. 4). This case where cross-diffusion effects are dominant displays different wave profiles compared with the case where both self-diffusion and cross-diffusion terms are present. Now, the oscillations attenuate slowly and are noticeable in the leading edges. They are present even in the core of the waves in the two peaks so that the two pulse peaks of the pulse pair become part of a whole oscillatory pattern [Figs. 4(a), 4(b), 4(d), 4(e), 4(g), and 4(h)], forming oscillatory multipeak pulses. These multiple waves are complemented by the pulse pair with strongly pronounced pulse peaks [Figs. 4(j)–4(l)] and also shown in three dimensions in Fig. 2], which also occurs in the first case of the model with both self-diffusion and cross-diffusion terms.

The multiwave regime of propagation is larger than described above. It also includes the coexistence of the simple standard solitary pulses with one peak. To demonstrate this feature, we show graphically an example of such waves in Fig. 5. The values of the model parameters  $D$ ,  $h$ , and  $a$  are chosen the same for both figures (Figs. 4 and 5 for the pulse pairs and the solitary pulses, respectively), which allows

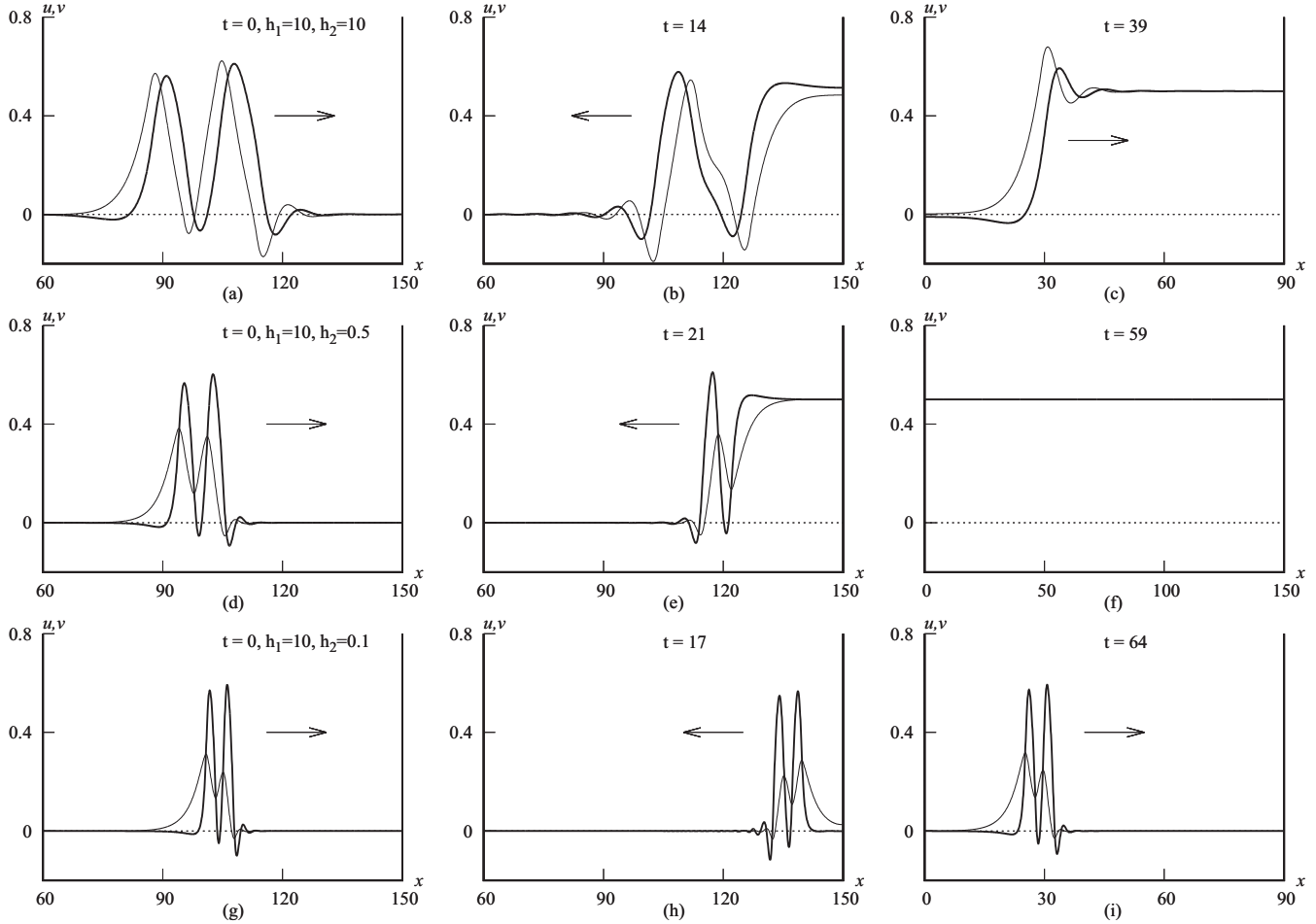


FIG. 8. Numerical simulations. Collision sequences and transformations of the multipulse waves with two peaks for the fixed value of  $h_1$  and different values of  $h_2$ . The activator  $u(x, t)$  and the inhibitor  $v(x, t)$  are shown in black and gray, respectively.

us to compare also the existence criteria for both types of waves. In the interval  $a \in (0, 0.25]$ , both the solitary pulses and the pulse pairs exist. For  $a = 0.26$  and larger values, the pulse pairs are absent, whereas the solitary pulses disappear only at  $a = 0.31$  and no longer exist for larger values of  $a$  [20]. Comparing the profiles of the solitary pulses and of the pulse pairs, we find that they are similar to each other. This observation can be explained by the same oscillatory character of the general solutions. The principal difference is related to the number of the coexisting waves in the multiwave regime: The solitary pulses appear as a single wave in the interval  $a \in (0, 0.25]$  [48], whereas multiple pulse pairs occur as mentioned above.

#### IV. MULTIPULSE WAVES

The results of numerical simulations for the propagation of the waves and their interaction with medium boundaries and each other are shown graphically in Figs. 6 and 7. The direct integration of the partial differential equations (3) has been performed on a one-dimensional medium of size  $L$ ,  $x \in [0, L]$  with Neumann boundary conditions for both variables  $u(x, t)$  and  $v(x, t)$ . We have applied a first-order time stepping scheme, which is fully explicit for the kinetic rate terms and fully implicit for the cross-diffusion terms. We

have considered only the case of pure cross diffusion, i.e., the self-diffusion coefficients vanish  $D = 0$ . We have used a second-order central difference approximation for the spatial derivatives. The space and time steps are chosen as  $\delta x = 0.02$  and  $\delta t = 0.00025$ , respectively. The initial conditions are as follows:

$$u(x, 0) = 0, \quad x \in [0, L], \quad (10)$$

and

$$v(x, 0) = \begin{cases} 0, & x \in [0, L/2], \\ v_0, & x \in (L/2, L] \end{cases} \quad (11)$$

see Figs. 6(a) and 7(a).

For a first set of numerical calculations, we chose the cross-diffusion coefficients to be  $h_1 = 10$  and  $h_2 = 0.002$  and started from the initial conditions (10) and (11). These conditions lead to the formation of two counterpropagating waves of pulse type with different numbers of core peaks dependent on the value of  $v_0$ , Figs. 6(b) and 7(b). The shapes of these waves are different for the activator  $u(x, t)$  and the inhibitor  $v(x, t)$ . The profile of the activator is similar to the bursting pattern, whereas it is saw shaped for the inhibitor. In other words, the activator is related to a *multipulse* wave, and the inhibitor corresponds to a *multipeak* pulse. The difference lies

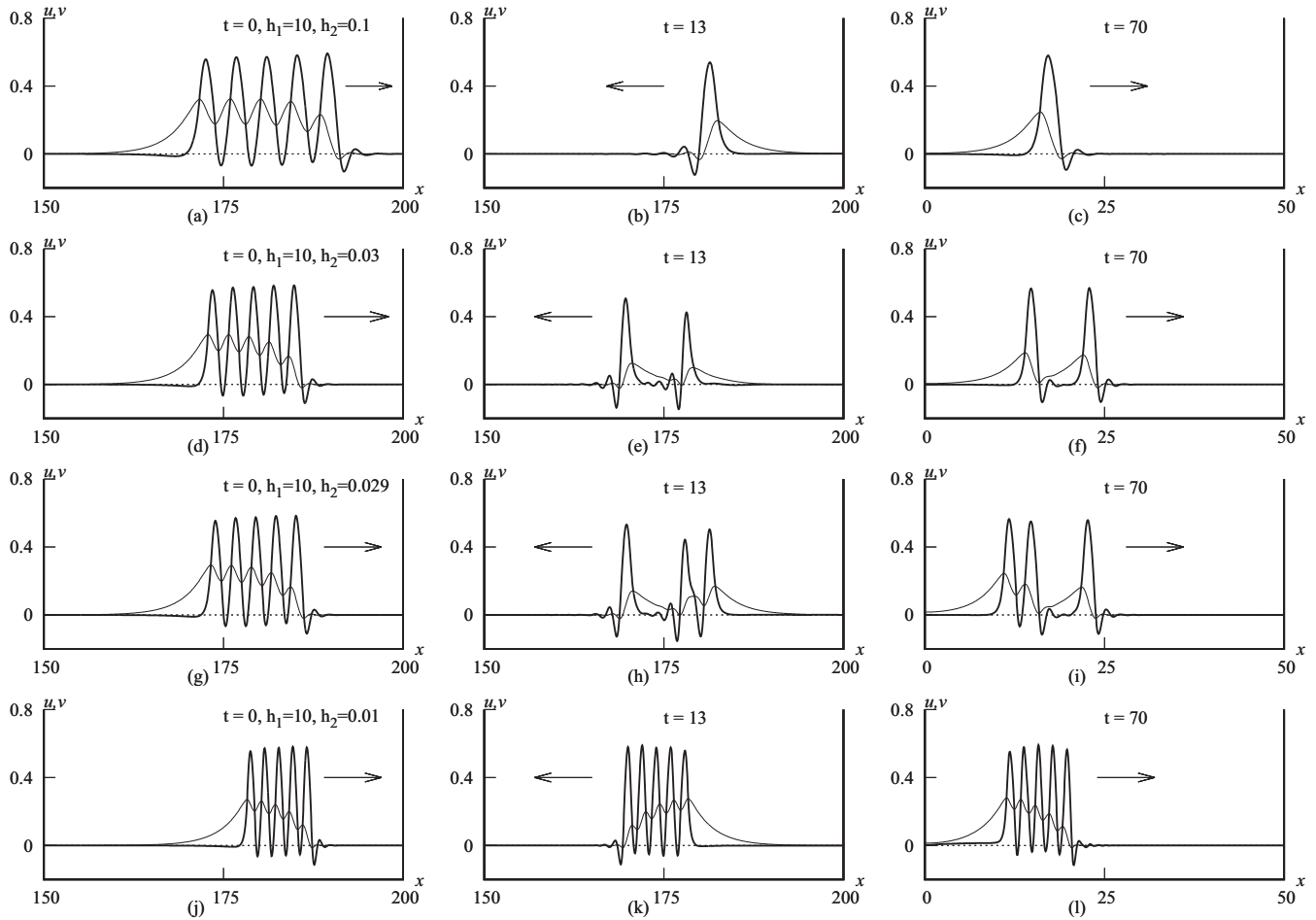


FIG. 9. Numerical simulations. Collision sequences and transformations of the multipulse waves with five peaks for the fixed value of  $h_1$  and different values of  $h_2$ . The activator  $u(x, t)$  and the inhibitor  $v(x, t)$  are shown in black and gray, respectively.

in the wells between the peaks in the core of the waves. The multipulse waves contain deep wells so that the peaks transform into pulses, whereas the multi-peak pulses have shallow wells in their core. These waves move towards the medium boundaries, reflect from them, keeping the same number of peaks, and travel towards each other [Figs. 6(c) and 7(c)]. They collide head on and pass through one another without changing their size and shape [Figs. 6(d) and 7(d)], i.e., they display soliton behavior. Therefore, for the sake of brevity, we call these multipulse waves with soliton interaction “*multipulses*.” Such soliton behavior of solitary pulses in reaction-diffusion systems with cross-diffusion terms of opposite signs has been reported before [11–14]. The difference is that we observe a *localized* sequence with a finite number of bound pulses, a finite pulse train, in contrast to periodic wave trains and solitary pulses studied previously. Note that these solitons in the reaction-diffusion system with cross diffusion [14] belong to the class of dissipative solitons [8,9].

In a second set of numerical calculations, we used the waves described above separately as new initial conditions in a medium with periodic boundary conditions. For these studies, the value of the second cross-diffusion coefficient was varied from  $h_2 = 0.002$  to  $h_2 = 10$ . The corresponding waves are shown in Figs. 6(e)–6(g) and 6(i)–6(k) and 7(e)–7(g) and 7(i)–7(k) for several values of  $h_2$ . As the value of the

cross-diffusion coefficient changes from  $h_2 = 0.1$  to  $h_2 = 10$ , the wells between the peaks in the core of the inhibitor waves become deeper, and the multi-peak pulse for the  $v$  variable transforms into a multipulse wave as for the  $u$  variable. At  $h_2 = 10$ , both waves, the activator and the inhibitor, belong to the multipulse type. When  $h_1 = h_2 = 10$  [Figs. 6(g) and 6(h)], the waves, composed of two bound pulses propagating with speed  $c = 5.93$ , agree qualitatively well with the analytically obtained paired-pulse waves with speed  $c \approx 5.936$  shown in Sec. III in Figs. 4(j)–4(l). Similar soliton pairs have been described in other nonlinear equations [49,50]. The numerical simulations show that the waves in Figs. 6 and 7 attain a steady profile asymptotically in time and are stable to low noises.

Multipulse collisions can exhibit other types of behavior, some of which are characteristic for dissipative systems. Figures 8 and 9 show the results of the interaction of the waves with the boundaries for the multipulse waves with two and five peaks, respectively. There exists a variety of wave transformations: the transition from the multipulse waves to pulse-front waves and further to the simple fronts [Figs. 8(a)–8(c)], the transition from the multipulse waves to pulse-front waves and further to annihilation [Figs. 8(d)–8(f)], the transition from the multipulse waves to solitary pulses [Figs. 9(a)–9(c)], and the transition from the multipulse waves to multipulse waves with a lower number of pulses [Figs. 9(d)–9(i)]. At some values



of the cross-diffusion coefficients, there are also solitonlike regimes [Figs. 8(g)–8(i) and 9(j)–9(l)]. For example, for the multipulse waves with two peaks, this behavior occurs when  $h_1 = 10$  and  $h_2 < 0.15$  or  $h_2 = 0.1$  and  $h_1 > 5$ .

Videos showing the wave propagation and interaction are provided in the Supplemental Material [51].

## V. SUMMARY

We have explored the effects of cross diffusion on various wave dynamics in the piecewise-linear FitzHugh-Nagumo equation, which has served for a long time in the literature as a paradigmatic reaction-diffusion model for excitable and bistable systems. We wish to emphasize our main result: In addition to the simple standard pulses, consisting of a single peak with growing and decaying edges, there occur sequences of bound traveling pulses, the finite wave trains

or *multipulse* waves in a bistable reaction-diffusion model of the FHN type with linear cross-diffusion terms describing attractive-repulsive interactions between the two species, such as pursuit-evasion interactions in a predator-prey system for example. In contradistinction to periodic wave trains, these multipulse waves possess a finite number of bound pulses in their sequence. We have found sequences consisting of two–five and seven bound pulses. We have shown that, for the inhibitor variable, the sequence of pulses transforms into one pulse with multiple peaks, called a *multipeak* pulse, when the values of the cross-diffusion constants differ significantly. We plan to extend our studies of multipulse waves to explore the possibility of pulses with peaks of a more complex shape.

We also investigated the interactions of the multipulse waves. We have discovered that, upon mutual collision, they pass through one another without any changes in their size and shape, demonstrating a soliton interaction. This characteristic property led us to call these waves *multipulsons*.

- 
- [1] A. Hagberg and E. Meron, Pattern formation in non-gradient reaction-diffusion systems: The effects of front bifurcations, *Nonlinearity* **7**, 805 (1994).
- [2] N. N. Rosanov and G. V. Khodova, Diffractive autosolitons in nonlinear interferometers, *J. Opt. Soc. Am. B* **7**, 1057 (1990).
- [3] T. Ohta and J. Kiyose, Collision of domain boundaries in a reaction-diffusion system, *J. Phys. Soc. Jpn.* **65**, 1967 (1996).
- [4] T. Ohta, J. Kiyose, and M. Mimura, Collision of propagating pulses in a reaction-diffusion system, *J. Phys. Soc. Jpn.* **66**, 1551 (1997).
- [5] N. J. Zabusky and M. D. Kruskal, Interaction of “Solitons” in a Collisionless Plasma and the Recurrence of Initial States, *Phys. Rev. Lett.* **15**, 240 (1965).
- [6] H. C. Tuckwell, Evidence of soliton-like behavior of solitary waves in a nonlinear reaction-diffusion system, *SIAM J. Appl. Math.* **39**, 310 (1980).
- [7] N. N. Rosanov, A. V. Fedorov, and G. V. Khodova, Effects of spatial distributivity in semiconductor optical bistable systems, *Phys. Stat. Solidi B* **150**, 545 (1988).
- [8] M. Bode and H.-G. Purwins, Pattern formation in reaction-diffusion systems—dissipative solitons in physical systems, *Physica D* **86**, 53 (1995).
- [9] H.-G. Purwins, H. U. Bödeker, and A. W. Liehr, in *Dissipative Solitons*, edited by N. Akhmediev and A. Ankiewicz, Lecture Notes in Physics Vol. 661 (Springer, Berlin, 2005), pp. 267–308.
- [10] B. S. Kerner and V. V. Osipov, Autosolitons, *Sov. Phys. Usp.* **32**, 101 (1989).
- [11] M. A. Tsyganov, J. Brindley, A. V. Holden, and V. N. Biktashev, Quasisoliton Interaction of Pursuit-Evasion Waves in a Predator-Prey System, *Phys. Rev. Lett.* **91**, 218102 (2003).
- [12] M. A. Tsyganov and V. N. Biktashev, Half-soliton interaction of population taxis waves in predator-prey systems with pursuit and evasion, *Phys. Rev. E* **70**, 031901 (2004).
- [13] M. A. Tsyganov, J. Brindley, A. V. Holden, and V. N. Biktashev, Soliton-like phenomena in one-dimensional cross-diffusion systems: A predator-prey pursuit and evasion example, *Physica D* **197**, 18 (2004).
- [14] O. Descalzi, N. Akhmediev, and H. R. Brand, Exploding dissipative solitons in reaction-diffusion systems, *Phys. Rev. E* **88**, 042911 (2013).
- [15] M. A. Tsyganov and V. N. Biktashev, Classification of wave regimes in excitable systems with linear cross diffusion, *Phys. Rev. E* **90**, 062912 (2014).
- [16] J. E. Truscott and J. Brindley, Equilibria, stability and excitability in a general class of plankton population models, *Philos. Trans. R. Soc. London Ser. A* **347**, 703 (1994).
- [17] V. K. Vanag and I. R. Epstein, Cross-diffusion and pattern formation in reaction-diffusion systems, *Phys. Chem. Chem. Phys.* **11**, 897 (2009).
- [18] V. N. Biktashev and M. A. Tsyganov, Solitary waves in excitable systems with cross-diffusion, *Proc. R. Soc. A* **461**, 3711 (2005).
- [19] E. P. Zemskov and A. Y. Loskutov, Oscillatory traveling waves in excitable media, *J. Exp. Theor. Phys.* **107**, 344 (2008).
- [20] E. P. Zemskov, I. R. Epstein, and A. Muntean, Oscillatory pulses in FitzHugh–Nagumo type systems with cross-diffusion, *Math. Med. Biol.* **28**, 217 (2011).
- [21] G. Gambino, M. C. Lombardo, and M. Sammartino, Pattern formation driven by cross-diffusion in a 2D domain, *Nonlin. Anal.: Real World Appl.* **14**, 1755 (2013).
- [22] G. Gambino, M. C. Lombardo, and M. Sammartino, Cross-diffusion-induced subharmonic spatial resonances in a predator-prey system, *Phys. Rev. E* **97**, 012220 (2018).
- [23] G. Gambino, M. C. Lombardo, G. Rubino, and M. Sammartino, Pattern selection in the 2D FitzHugh–Nagumo model, *Ricerche Math.* **68**, 535 (2019).
- [24] I. Berenstein and C. Beta, Spatiotemporal chaos arising from standing waves in a reaction-diffusion system with cross-diffusion, *J. Chem. Phys.* **136**, 034903 (2012).
- [25] I. Berenstein and C. Beta, Cross-diffusion in the two-variable Oregonator model, *Chaos* **23**, 033119 (2013).
- [26] G. Gambino, M. C. Lombardo, and M. Sammartino, Turing instability and traveling fronts for a nonlinear reaction–diffusion system with cross-diffusion, *Math. Comp. Simul.* **82**, 1112 (2012).

- [27] F. S. Berezovskaya, A. S. Novozhilov, and G. P. Karev, Families of traveling impulses and fronts in some models with cross-diffusion, *Nonlin. Anal.: Real World Appl.* **9**, 1866 (2008).
- [28] F. Berezovskaya, E. Camacho, S. Wirkus, and G. Karev, “Traveling wave” solutions of FitzHugh model with cross-diffusion, *Math. Biosci. Eng.* **5**, 239 (2008).
- [29] F. Berezovskaya, in *Mathematical Sciences with Multidisciplinary Applications*, Springer Proceedings in Mathematics & Statistics Vol. 157, edited by B. Toni (Springer, Cham, 2016), pp. 1–20.
- [30] E. P. Zemskov, M. A. Tsyganov, and W. Horsthemke, Oscillatory pulses and wave trains in a bistable reaction-diffusion system with cross diffusion, *Phys. Rev. E* **95**, 012203 (2017).
- [31] E. P. Zemskov, M. A. Tsyganov, and W. Horsthemke, Oscillatory pulse-front waves in a reaction-diffusion system with cross diffusion, *Phys. Rev. E* **97**, 062206 (2018).
- [32] R. FitzHugh, Impulses and physiological states in theoretical models of nerve membrane, *Biophys. J.* **1**, 445 (1961).
- [33] J. Nagumo, S. Arimoto, and S. Yoshizawa, An active pulse transmission line simulating nerve axon, *Proc. IRE* **50**, 2061 (1962).
- [34] B. van der Pol, On relaxation-oscillations, *Philos. Mag.* **2**, 978 (1926).
- [35] K. F. Bonhoeffer, Über die Aktivierung von Passivem Eisen in Salpetersäure, *Z. Elektrochem. Angew. Phys. Chem.* **47**, 147 (1941).
- [36] K. F. Bonhoeffer, Activation of passive iron as a model for the excitation of nerve, *J. Gen. Physiol.* **32**, 69 (1948).
- [37] A. L. Hodgkin and A. F. Huxley, A quantitative description of membrane current and its application to conduction and excitation in nerve, *J. Physiol.* **117**, 500 (1952).
- [38] H. P. McKean, Nagumo’s equation, *Adv. Math.* **4**, 209 (1970).
- [39] J. Rinzel and J. B. Keller, Traveling wave solutions of a nerve conduction equation, *Biophys. J.* **13**, 1313 (1973).
- [40] J. Rinzel and D. Terman, Propagation phenomena in a bistable reaction-diffusion system, *SIAM J. Appl. Math.* **42**, 1111 (1982).
- [41] A. Ito and T. Ohta, Self-organization in an excitable reaction-diffusion system. III. Motionless localized versus propagating-pulse solutions, *Phys. Rev. A* **45**, 8374 (1992).
- [42] V. Méndez and J. Camacho, Dynamics and thermodynamics of delayed population growth, *Phys. Rev. E* **55**, 6476 (1997).
- [43] V. Méndez and J. E. Llebot, Hyperbolic reaction-diffusion equations for a forest fire model, *Phys. Rev. E* **56**, 6557 (1997).
- [44] G. Abramson, A. R. Bishop, and V. M. Kenkre, Effects of transport memory and nonlinear damping in a generalized Fisher’s equation, *Phys. Rev. E* **64**, 066615 (2001).
- [45] V. Méndez, S. Fedotov, and W. Horsthemke, *Reaction-Transport Systems* (Springer, Heidelberg, 2010).
- [46] V. N. Biktashev and M. A. Tsyganov, Envelope Quasisolitons in Dissipative Systems with Cross-Diffusion, *Phys. Rev. Lett.* **107**, 134101 (2011).
- [47] E. P. Zemskov, K. Kassner, and M. J. B. Hauser, Wavy fronts and speed bifurcation in excitable systems with cross diffusion, *Phys. Rev. E* **77**, 036219 (2008).
- [48] There exists also a single solitary pulse with negative speed. It is the counterpart to the  $c > 0$  wave with an inverted  $\xi \rightarrow -\xi$  profile and the same absolute value of speed.
- [49] A. G. Vladimirov, G. V. Khodova, and N. N. Rosanov, Stable bound states of one-dimensional autosolitons in a bistable laser, *Phys. Rev. E* **63**, 056607 (2001).
- [50] J. M. Soto-Crespo, Ph. Grelu, N. Akhmediev, and N. Devine, Soliton complexes in dissipative systems: Vibrating, shaking, and mixed soliton pairs, *Phys. Rev. E* **75**, 016613 (2007).
- [51] See Supplemental Material at <http://link.aps.org/supplemental/10.1103/PhysRevE.101.032208> for numerical simulations of wave propagation.